COMPDYN 2011
3rd ECCOMAS Thematic Conference on
Computational Methods in Structural Dynamics and Earthquake Engineering
M. Papadrakakis, M. Fragiadakis, V. Plevris (eds.)
Corfu, Greece, 25–28 May 2011

DEVELOPING FRAGILITY CURVES FOR A TYPICAL PILE-SUPPORTED WHARF STRUCTURE

Abdollah Shafieezadeh[1], Reginald DesRoches[2], and Karthik Ramanathan[3]

[1] Georgia Institute of Technology,
School of Civil & Environmental Engineering, 790 Atlantic Drive, Atlanta GA 30332
a.shafiee@gatech.edu

[2] Georgia Institute of Technology,
School of Civil & Environmental Engineering, 790 Atlantic Drive, Atlanta GA 30332
reginald.desroches@ce.gatech.edu

[3] Georgia Institute of Technology,
School of Civil & Environmental Engineering, 790 Atlantic Drive, Atlanta GA 30332
karthik.ramanathan@ce.gatech.edu

Keywords: Ports, Seismic Risk Assessment, Fragility Analysis, Nonlinear Dynamic Analysis

Abstract. *Container wharves are one of the main components in port systems which are susceptible to structural damage during seismic events. Since regional economies depend largely on the operation of port systems, assessment of the vulnerability of these systems to seismic events is crucial. Seismic risk analysis provides a framework to estimate potential economic losses by incorporating the available information on structure details, soil conditions, repair cost for different components, etc. This paper studies the fragility of wharf structures for a typical pile-supported wharf as part of the NEES-GC project, Seismic Risk Mitigation of Strategic Ports. For this purpose, a two dimensional detailed model is developed for a typical pile-supported wharf structure on the west coast of the United States. The modeled structure contains a pile-deck connection model calibrated to experimental results, pile elements with spread plasticity capability and fiber sections, and soil-structure interaction elements capable of liquefaction modeling. Based on experts opinion and experimental results, a set of limit states are considered for a number of critical components of the wharf structure whose damage induce a disruption in the normal operation of ports. Using the nonlinear model and the limit states, a set of fragility curves are developed for 63 ground deformations generated for this study. The outcome of this research will help port owners to indicate the most vulnerable components of port infrastructures and invest the limited retrofit resources for risk mitigation of ports.*

1 INTRODUCTION

Seaports are intermodal transfer points in transportation networks which have a major role in the regional economy. The physical activities of ports i.e. loading and unloading of cargo, raw materials, etc are concentrated in a small geographic area and therefore, any disruption in the normal performance of structural and geotechnical components of ports may lead to partial or even full disruption of the commercial activities of the port. Historical cases of seaport damage have shown that any disruption in the activities of port infrastructures may lead to significant direct and secondary losses. Particularly poignant examples were the 1995 Kobe earthquake and 2010 Haiti earthquake in which liquefaction and lateral spreading of embankments imposed severe damage to both structural and non-structural components of ports [1,2]. Seismic risk analysis as a key component in risk mitigation efforts provides a framework to estimate potential economic losses by incorporating the available information on structure details, soil conditions, repair cost for different components, etc. In general, seismic risk of a system can be decomposed into a number of components among which is the fragility of the system. The fragility of a wharf model defines the probability of occurrence of various damage states as a function of the firm-site ground motion.

Despite the importance of ports and their vulnerability to seismic damage, a limited number of researches studied the fragility of wharves to seismic events [3,4]. The present study focuses on developing fragility curves for a typical pile supported wharf with batter piles in the west coast of the United States. This is accomplished by incorporating realistic representations of the nonlinear behavior of pile elements, nonlinear force-deformation characteristics of pile-deck connections, and nonlinear dynamic pile-soil interactions in liquefaction susceptible soils. Based on experts' opinion and experimental results, a set of limit states are considered for a number of components of the wharf structure which their damage induces a disruption in the normal operation of ports. Using the nonlinear model and the limit states, a set of fragility curves are developed for 63 ground deformations of the soil embankment and pore water pressure generated for this study through free-field analysis.

2 NUMERICAL MODELING OF A TYPICAL PILE-SUPPORTED WHARF

2.1 Structural Elements

A typical pile supported wharf in the west coast of the United States is modeled in this study. The Finite Element (FE) model of the wharf is developed in OpenSees, an object-oriented FE analysis framework [5]. The transverse section of the wharf is shown in Figure 1. Directions parallel and normal to the landside-seaside direction in the plane of the wharf deck are defined as transverse and longitudinal directions, respectively. In the longitudinal direction, wharves consist of repeating segments, referred to as strips, which are used to represent the wharf in two dimensions. The deck of the wharf and the landside crane rail are supported by pre-stressed vertical and batter piles (Figure 1). The pre-stressed piles are modeled by force-based nonlinear beam-column elements [6,7] with fiber cross-sections. The piles and the deck are connected by T-headed dowel bars which is a common connection for wharf structures. In the FE model of the wharf, these connections are modeled by a link element at the top of pre-stress piles. In order to capture the nonlinear force-deformation characteristics of pile-deck connections, the implemented procedure is calibrated with the result of a full scale test conducted by Lehman et al. [8].

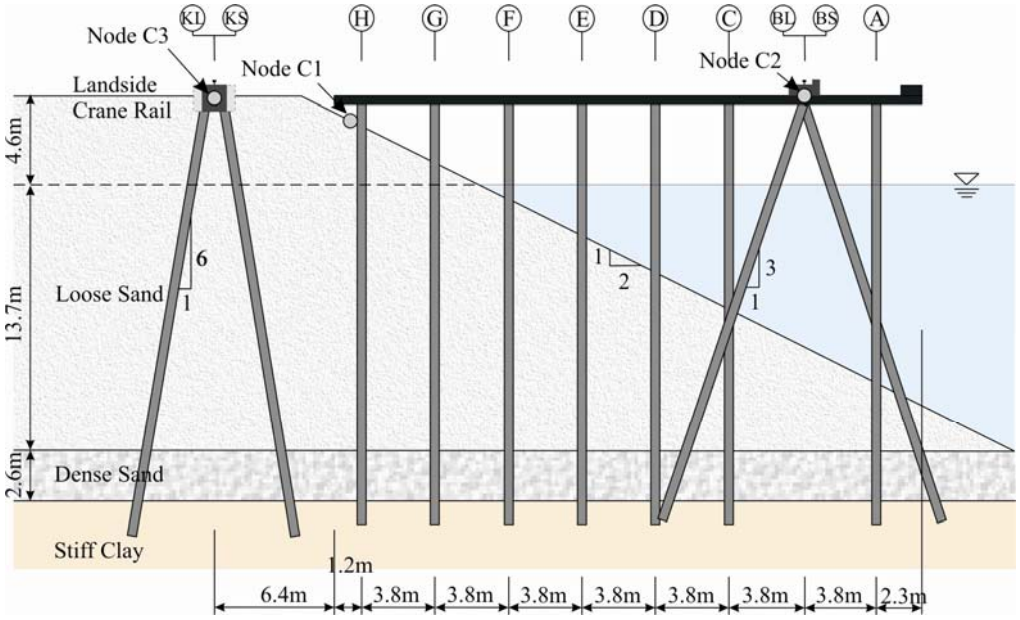

Figure 1. Configuration of the wharf and landside crane rail

2.2 Geotechnical Considerations

The profile of the soil at the location of the wharf is shown in Figure 1 which consists of three layers: a layer of loose sand in the top 18.3 m underlain by a layer of dense sand with a thickness of 2.6 m on top of a layer of clay. The water level is 4.6 m from the soil surface on the landside. Soil properties of the three layers including mass density, shear modulus, Poisson's ratio, friction angle, and undrained shear strength are presented in Table 1.

Pile-soil interaction in the horizontal direction is modeled by a series of nonlinear soil springs including macroelements [9] and conventional p-y springs [10] in sand and clay layers respectively. In the vertical direction, t-z and q-z springs are implemented to model the resistance in the face and end of the piles respectively. Soil springs are assigned at every 1 m in depth from the soil surface and their associated material properties are found for the corresponding soil layer.

Soil layer	γ (gr/cm3)	G (MPa)	ν	φ (deg)	cu (kPa)
Loose Sand	1.85	80	0.2	34	-
Dense sand	2.05	120	0.2	38	-
Clay	1.75	100	0.4	-	48

Table 1. Soil layers properties.

3 GROUND MOTIONS

Generating PSDMs for critical response measures of the wharf requires selection of representative ground motions as the inputs for nonlinear time-history analysis. A total of 63 empirical (i.e., observed) and simulated ground motions have been selected to represent a broad range of possible earthquake magnitudes and distances. The soil condition for these ground motions is typical of firm soils in coastal California. Among 63 ground motions, fifty six ground motion time-histories are empirical which are selected from the database used to de-

velop the Next Generation Attenuation of Ground Motions (NGA) project [11]. This suite of ground motions is selected randomly from the database such that all of the earthquakes have minimum moment magnitude (Mw) of 5.5 and closest distance to the rupture (R) of 0 to 60 km. All of the selected ground motions are earthquakes within the United States except for the 1995 Kobe, Japan and 1999 Chi‐Chi, Taiwan earthquakes. Furthermore, seven simulated ground motions are added to the bin to represent large magnitude California earthquakes which are not present in the NGA database. The resulting bin of empirical and simulated ground motions covers a broad range of earthquake scenarios in terms of minimum moment magnitude and the closest distance to rupture. Figure (2) presents M_w versus R for the suit of sixty three earthquakes considered in this study.

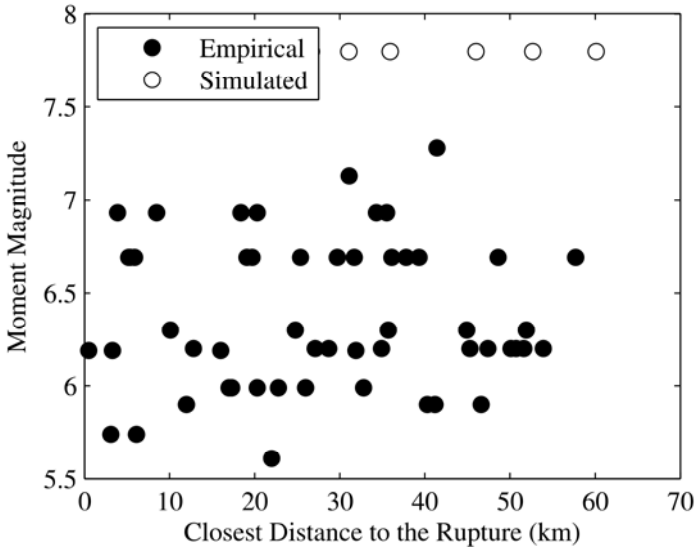

Figure 2. Moment magnitude vs. the closest distance to rupture.

The selected ground motions are used as input for numerical models of the soil embankments supporting the wharf-foundation. The nonlinear coupled ground deformation and transient pore pressure response of the wharf embankment to input ground shakings are numerically evaluated by Vytiniotis et al. [12]. The analysis uses the advanced elasto-plastic effective stress soil model proposed by Dafalias and Manzari [13]. This model is able to realistically capture the stress-strain behavior of sand during cyclic mobility events. More details about the model and assumptions together with numerical results can be found in Vytiniotis et al. [12]. Soil deformations and excess pore water pressure ratios in sand layers in the horizontal direction are applied to the far-field end of the macroelement, while for other soil springs only soil deformations are input to the model. The dynamic response of the foundation-wharf-crane system is found for time-histories of ground deformation and pore pressures within the surrounding soil medium.

4 FRAGILITY ANALYSIS FRAMEWORK

A key component in predicting the damage of a structural system when subjected to an earthquake with expected characteristics is the fragility of the system. A fragility curve describes the probability that the structure fails to satisfy a prescribed performance criterion

conditioned on a seismic intensity measure (*IM*) representative of the seismic loading. In structural engineering community, it is common to define the event of a structure failing to meet a performance requirement called damage state by simply the case where demand (*D*) exceeds capacity (*C*); i.e. *C*<*D*. Assuming that both capacity and demand can be described by lognormal distributions, the probability of the structure exceeding a particular damage state for a given *IM* in closed form is

$$P(C < D \mid IM) = 1 - \Phi\left(\frac{\ln(m_C) - \ln(m_D)}{\sqrt{\beta_C^2 + \beta_D^2}}\right) \tag{1}$$

in which Φ(.) is the standard normal distribution and m and β are the median and logarithmic standard deviation respectively.

According to Equation (1), evaluation of the seismic fragilities of structures requires developing models for demand on the structural components using nonlinear time-history analysis of the wharf-foundation system as well as capacity model for the critical components.

4.1 Probabilistic seismic demand models

One of the constitutive components of the conditional probability of failure in Equation (1) is the demand model for which a probabilistic analysis is required to determine the parameters m_D and β_D. Cornell et al. [14] showed that seismic median drift demands can be represented well as a power function of *IM*.

$$m_D = a(IM)^b \tag{2}$$

where *a* and *b* are constants determined by a simple linear regression analysis of the seismic demand in the transformed logarithmic space in the following form.

$$\ln(m_D) = \ln(a) + b\ln(IM) \tag{3}$$

The assumption of demand following a lognormal distribution with respect to the IM is applied to all demand measures associated with critical wharf components including the curvature of piles and pile-deck connections and the relative displacement of the structurally separated landside crane rail with respect to the wharf. Assuming that the dispersion of seismic demand parameters is independent from the IM in the logarithmic scale, the uncertainties in the seismic demand parameters β_D in Equation (1) is determined as the logarithmic standard deviation of errors in fitting the demand models as follows.

$$\beta_D = \sqrt{\frac{\sum_{i=1}^{n}\left(\ln(D_i) - \ln\left(aIM^b\right)\right)^2}{n-2}} \tag{4}$$

Subjecting the wharf-foundation to time-histories of ground deformation and pore water pressures of the embankment soil, the dynamic response of the wharf is found using nonlinear time-history analysis and the maximum response in critical response measures are recorded. This study uses peak ground acceleration (PGA) as the *IM* which is a widely used *IM* in earthquake engineering community.

Figure (3) shows the seismic demand of the piles and pile-deck connections in terms of curvature and the relative displacement of the landside crane rail and wharf in the horizontal direction as a function of PGA. It is observed that the assumption of independence of the demand from intensity measure in the logarithmic scale is almost valid for all demand parame-

ters. Furthermore all of the demand parameters are seen to be reasonably well described by a linear regression in the log scale which validates the assumption of demand be lognormally distributed.

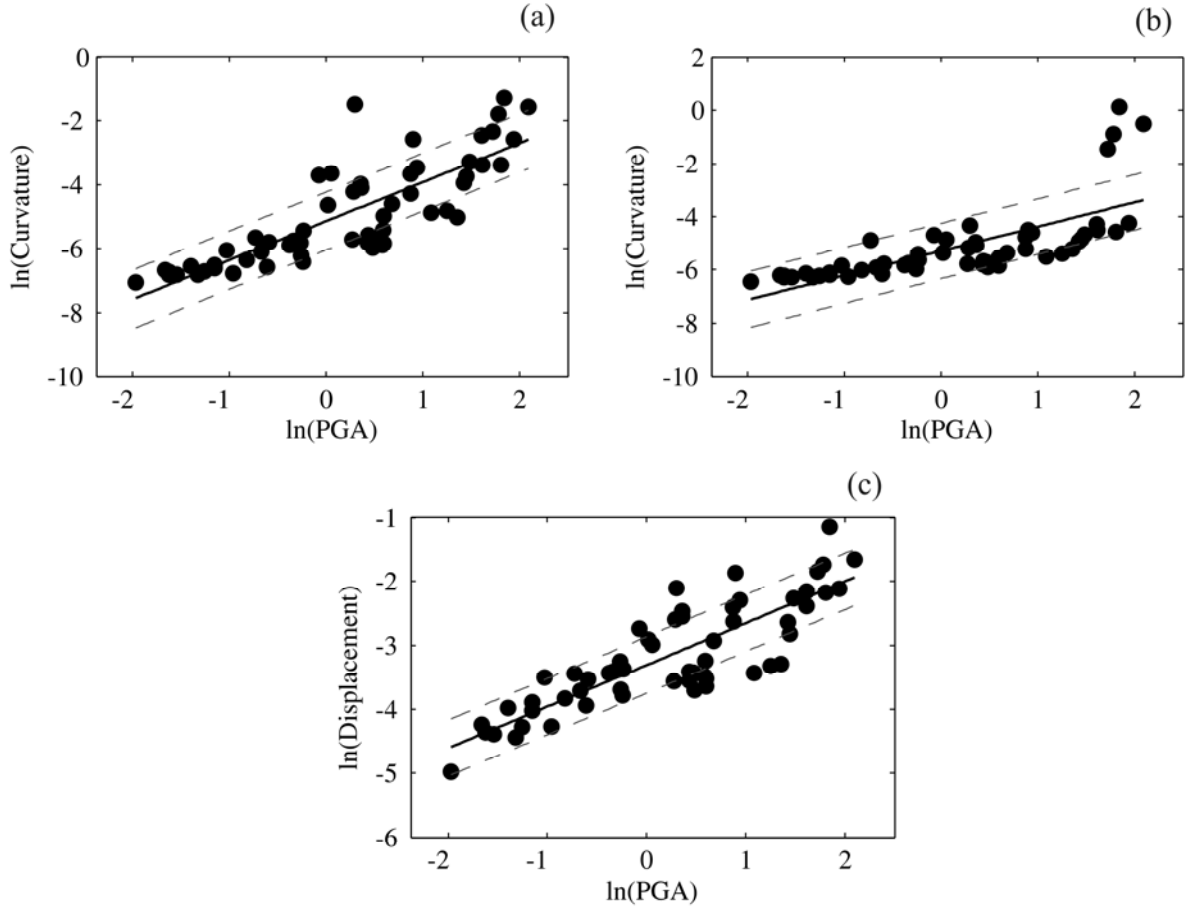

Figure 3. Probabilistic seismic demand models for (a) pile-deck connections, (b) pile sections, and (c) relative movement of the wharf with respect to the landside crane rail.

4.2 Component limit states

The study uses three damage states: slight, moderate, and extensive in which the first two states are adopted from PIANC [15]. The slight damage state has a high probability of occurrence during the life time of the wharf in which no structural damage is permitted. The moderate damage has a lower probability of occurrence compared to the slight damage state in which only reparable damages and limited residual deformations are allowed. Because of the mutual exclusiveness property of the damage states, all other damages that are more severe and consequently less probable than the ones associated with the moderate damage state falls into the extensive damage state category.

A number of response measures of the wharf that are critical in the overall structural response of the wharf and the performance of associated components such as cranes are considered in this study. As mentioned before, these critical response measures are the curvature of piles and pile-deck connections and the relative displacement of the wharf with respect to the landside rail. The limit states associated with these responses are assumed to be lognormally distributed.

The median m_C of the capacity limit state for the pile-deck connections is obtained from the experimental test conducted by Lehman et al. [8] in which the provided drift limits are converted to curvature limits at the connection using numerical simulation of the test specimen.

The curvature limit states for different pile sections are found using moment-curvature analyses. Typically the cross-section of a pile contains all or a number of the following discretized sub-regions, the cover layer of unconfined concrete, the inner core region of confined concrete, the circular layer of longitudinal reinforcing steel, and the circular layer of prestressing strands. In order to determine the median deformation capacity of the piles, the strain limits of the constitutive section materials provided by PIANC [15] are used to determine the corresponding section curvature. The strain limits, for each of the constitutive materials are presented in Table (2).

	Limit State		
Material Response	Slight	Moderate	Severe
Concrete extreme fiber compression strain	0.004	0.008	–
Core concrete extreme fiber compression strain	–	–	2/3 ε_{cu}
Reinforcing Steel tension strain	0.01	0.01	2/3 ε_{su}
Prestressing strand incremental strain	0.005	0.015	2/3 ε_{pu}

Table 2. Strain limits associated with defined limit states for constitutive materials of pre-stress pile sections

Performing moment-curvature analyses for different sections of the pre-stressed piles in the wharf configuration, the curvature limits are determined as the minimum of the curvatures corresponding to the strain limits of different constitutive section materials for each limit state. The derived curvature limits for all sections in the wharf are presented in Figure (4). The median of the curvature limit of different pile sections in each limit state is considered as the median m_C of the capacity limit state.

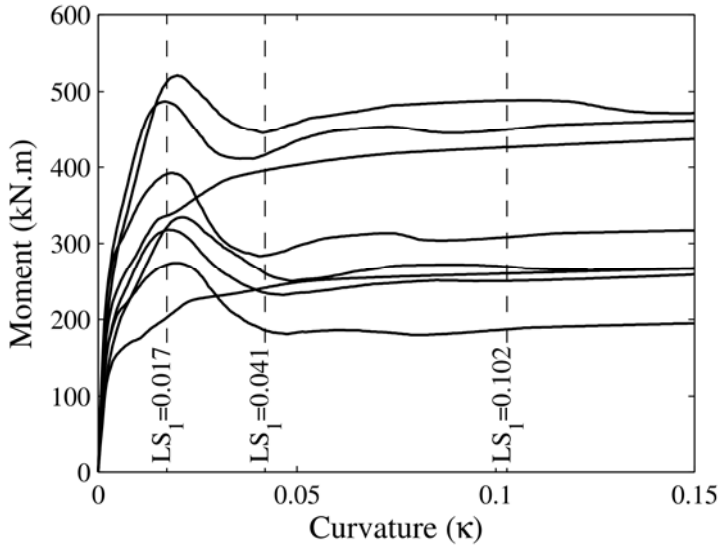

Figure 4. Moment curvature curves of different sections of the piles and the median limit states.

The median of the limit states m_C for the relative movement of the landside crane rail with respect to the wharf is provided by Werner and Cook [16] based on expert opinion. The sum-

mary of deformation limits of different wharf components associated with three limit states chosen for this study are presented in Table (3).

	Limit State		
Component	Slight	Moderate	Severe
Pile-deck connection rotation (1/m)	0.007	0.035	0.08
Pile section curvature (1/m)	0.017	0.041	0.102
Relative displacement of the landside rail with respect to wharf deck (cm)	0.3	2.5	15.2

Table 3. The deformation limits of critical wharf components corresponding to the chosen limit states.

4.3 Component fragility curves

After developing the probabilistic seismic demand models and determining the corresponding limit states of the wharf damage for the critical components, the component fragilities are constructed using the closed form given in Equation (1). Following Ellingwood [17], the dispersion in the capacity is assumed 0.2 while the dispersion in the demand is found from Equation (4).

The resulting fragility curves for pile sections, pile-deck connections and the relative displacement of the landside crane rail with respect to the wharf are shown in Figure (5)

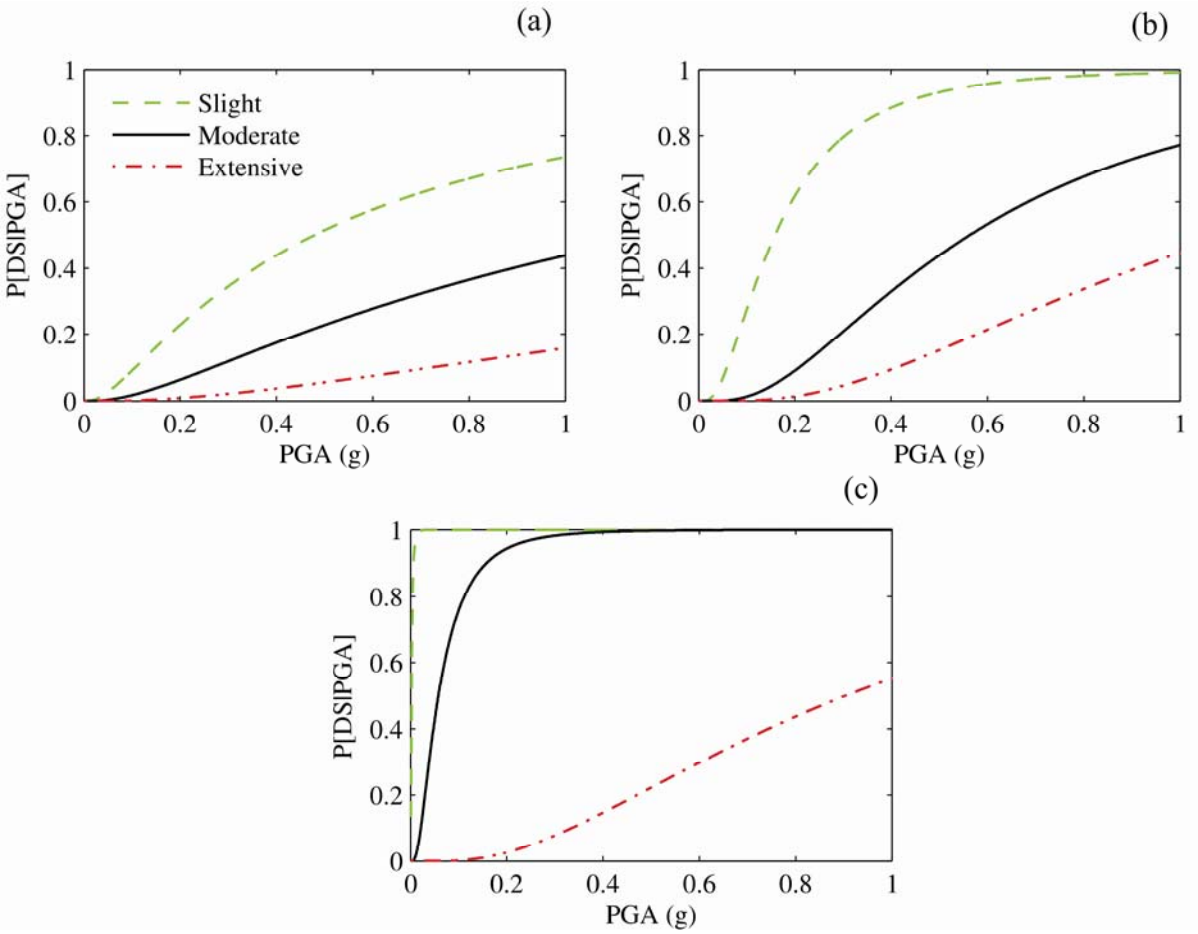

Figure 5Seismic fragility curves for (a) pile-deck connections, (b) pile sections, and (c) relative movement of the wharf with respect to the landside crane rail.

respectively. It is observed that pile-deck connections are less susceptible to damage compared to pile sections for the same intensity measure i.e. PGA. This is in large due to the considerable relative deformation of the loose and dense sand layers (Figure 1) as a result of liquefaction of the embankment. This consequently imposes large curvature demands on pile sections close to the interface of soil layers. Furthermore, the wharf damage as a result of excessive relative displacement of the wharf with respect to the structurally separated landside crane rail is seen to by highly probable. This response measure of the wharf has a large impact on the operation of the container cranes, and therefore requires more attention. A possible retrofit measure for the excessive relative displacement of the wharf can be connecting the separate landside rail and wharf using reinforced concrete.

5 CONCLUSIONS

This study presents the analytical fragility analysis of a typical pile supported wharf in the west coast of the United States. The two dimensional numerical model of the wharf used for developing fragility curves includes realistic representation of the critical wharf components including piles, pile-deck connections, and soil springs for liquefiable soils. The ground motions for time-history analysis represent a broad range of earthquake scenarios in terms of moment magnitude and the closest distance to rupture. The study presents the results of the nonlinear time-history analysis of the wharf-foundation system and the associated probabilistic seismic demand models for the ground deformations and pore water pressures of the surrounding soil medium for various seismic hazard scenarios. Using the analytical relations for the conditional probability of exceeding defined damage states, a set of fragility curves are developed for critical wharf components including piles, pile-deck connections, and the relative displacement of the landside crane rail and the wharf. It was found that the relative displacement of the wharf with respect to the structurally separated landside crane rail is the most vulnerable component in the wharf response. Furthermore, pile sections were found to be more susceptible to damage compared to pile-deck connections.

REFERENCES

[1] S.D. Werner, S.E. Dickenson, *Hyogo-Ken Nanbu earthquake of January 17, 1995: a post-earthquake reconnaissance of port facilities*. American Society of Civil Engineers, 1996.

[2] M. Eberhard, S. Baldridge, J. Marshall, W. Mooney, G.J. Rix, *The mw 7.0 Haiti Earthquake of Jauary 12, 2010, V. 1.0,* USGS/EERI Advance Reconnaissance Team Report, 2010.

[3] U.J. Na, S.R. Chaudhuri, M. Shinozuka, Performance evaluation of pile-supported wharf under seismic loading. A.K.K. Tang and S.D. Werner eds. *Lifeline Earthquake Engineering in a Multihazard Environment (TCLEE 2009)*, Oakland, USA, 2009.

[4] R.W. Boulanger, C.J. Curras, B.L. Kutter, D.W. Wilson, Seismic soil-pile-structure interaction experiments and analyses. *Journal of Geotechnical and Geoenvironmental Engineering*, **125**, 750–759, 1999.

[5] F. McKenna, M.H. Scott, G.L. Fenves, Nonlinear finite-element analysis software architecture using object composition. *Journal of Computing in Civil Engineering*, **24**, 95–107, 2010.

[6] E. Spacone, F.C. Filippou, F.F. Taucer, Fiber beam-column model for non-linear analysis of R/C frames: part I. Formulation. *Earthquake Engineering & Structural Dynamics,* **25**, 711–725, 1998.

[7] R.M. De Sousa, *Force-based finite element for large displacement inelastic analysis of frames.* Ph.D. Thesis, Department of Civil Engineering, University of California, Berkeley, CA, 2000.

[8] D.E. Lehman, E. Brackmann, A. Jellin, C.W. Roeder, Seismic performance of pile-wharf connections. A.K.K. Tang and S.D. Werner eds. *Lifeline Earthquake Engineering in a Multihazard Environment (TCLEE 2009)*, Oakland, USA, 2009.

[9] Varun, D. Assimaki, A nonlinear dynamic macroelement for soil-structure interaction analyses of pile-supported waterfront structures. *International Journal for Numerical and Analytical Methods in Geomechanics*, In Press, 2010.

[10] R.W. Boulanger, C.J. Curras, B.L. Kutter, D.W. Wilson, Seismic soil-pile-structure interaction experiments and analyses. *Journal of Geotechnical and Geoenvironmental Engineering*, **125**, 750–759, 1999.

[11] B. Chiou, R. Darragh, N. Gregor, W. Silva, NGA project strong-motion database. *Earthquake Spectra*, **24**, 23-44, 2008.

[12] A. Vytiniotis, A.J. Whittle, E. Kausel, Effects of seismic motion characteristics on cyclic mobility and liquefaction. 5th International Conference on Earthquake Geotechnical Engineering, Santiago, Chile, January 10-13, 2011.

[13] Y.F. Dafalias and M.T. Manzari, Simple plasticity sand model accounting for fabric change effects. *Journal of Engineering Mechanics*, **130**, 622-634, 2004.

[14] A.C. Cornell, F. Jalayer, R.O. Hamburger, and D.A. Foutch, Probabilistic basis for 2000 SAC Federal Emergency Management Agency Steel Moment Frame Guidelines. *Journal of Structural Engineering*, **128**, 526-532, 2002.

[15] International Navigation Association (PIANC). *Seismic design guidelines for port structures*. A.A. Balkema Publishers, 2001.

[16] S.D. Werner and W.C. Cook, Wharf repair estimates for use in demonstration seismic risk analysis of port systems, Prepared for NEES-GC Project: Seismic Risk Mitigation of Port Systems, September 17, 2009.

[17] B.R. Ellingwood, O.C. Celik, K. Kinali, Fragility assessment of building structural systems in Mid-America, *Earthquake Engineering and Structural Dynamics*, **36**, 1935-1952, 2007.